*Journal of Metals, Materials and Minerals, Vol. 32, No. 4, pp. 186-193, 2022*

# Magnetic nanoparticles coated with zwitterionic copolymer as an advanced material for rapid and instrument-free biomolecular detection in human serum

Supannika BOONJAMNIAN[1], Varunee SADSRI[1], Voravee P. HOVEN[3,4], and Piyaporn NA NONGKHAI[1,2,*]

[1] *Research Unit for Sensor Innovation (RUSI), Burapha University, Chon Buri 20131, Thailand.*
[2] *Department of Chemistry and Center of Excellence for Innovation in Chemistry, Faculty of Science, Burapha University, Chon Buri 20131, Thailand*
[3] *Department of Chemistry, Faculty of Science, Chulalongkorn University, Bangkok 10330, Thailand*
[4] *Center of Excellence in Materials and Biointerfaces, Chulalongkorn University, Bangkok 10330, Thailand*

***Corresponding author e-mail:** piyapornn@buu.ac.th

**Received date:**
31 August 2022
**Revised date**
25 November 2022
**Accepted date:**
19 December 2022

**Keywords:**
Magnetite nanoparticles;
Zwitterionic copolymer;
Medical diagnostics;
Agglutination assay

**Abstract**

The traditional agglutination assays especially those based on polystyrene beads have been recognized as convenient tools for disease diagnosis despite their limited detection range and low sensitivity. Unlike other particles namely polystyrene beads, $SiO_2$ and gold nanoparticles having insignificant magnetic properties, magnetic nanoparticles (MNPs) offer unique advantages as their magnetic properties for agglutination methods. In the presence of magnet, not only can they be used to enrich the samples, but also their aggregation can also be induced, providing sensitive and rapid measurements. This work aims to develop MNPs for aggregation-based biomolecular detection. The MNPs were surface-modified with PMAMPC via an in situ coating method, then biotin as the target-specific probe was immobilized. The biotin-conjugated PMAMPC-MNPs were used for capturing and detecting the complementary protein, streptavidin in human serum samples. With the magnetic-induction, the nanoparticles would aggregate in the presence of streptavidin, resulting in a short detection time even in undiluted human serum. The concentration range for the detection was 35 nM to 150 nM and the lowest concentration of detection was 35 nM or equivalent to 2.5 $mg{\cdot}mL^{-1}$. The fact that this is simple, rapid and instrument-free method for biomolecular detection broadens their potential use in a variety of diagnostic applications.

## 1. Introduction

The detection of specific biological molecules such as protein biomarkers, pathogens and cells in biological fluid is especially important in medical diagnosis due to their potential as an indicator for the early prediction of diseases [1-6]. Several commonly used techniques for biological molecule detection involve inconvenient and time-consuming procedures as well as specialized equipments such as electrochemical instruments [2], quartz crystal microbalance (QCM) [3], mass spectrometry (MS) [4], and surface plasmon resonance (SPR) [5,6]. Thus there is still a need for new diagnostic tools that can be rapidly and easily deployed.

The aggregation of particles via specific interactions between complementary biological components has gained increasing attention in medical diagnosis due to its simplicity, practicality, and low cost [7-16]. Traditionally, agglutination assays based on polystyrene nano- and microspheres, well-known as the latex agglutination test, have been extensively used. Specific monoclonal antibodies as capture probes for specific detection of the corresponding antigen are coated on particles, causing the aggregation of the particles which can be detected by naked eye. However, the sensitivity of these assays in blood serum is relatively low compared with the instrumental methods. Due to the hydrophobic surface of polystyrene particles, non-specific adsorption of proteins and other biological components is often found, causing a high background signal which significantly affects the selectivity and sensitivity of the detection.

Magnetic nanoparticles (MNPs) have recently received much attention in biomolecular detection [13-26]. Iron oxide nanoparticles, such as magnetite nanoparticles ($Fe_3O_4$NPs), are commonly used for the synthesis of MNPs. Their inherit magnetic response enables them to be manipulated in the presence of an external magnetic field. Additionally, their surfaces can be easily modified [26]. Polymer coating on MNPs is a well-known and efficient approach that can improve their stability and biocompatibility as well as their hydrophilicity and conjugating capability [13,18,19,21,25,26]. In particular, coating with polymers having antifouling characteristics also resist non-specific adsorption, providing highly selective and sensitive detection. Although the magnetic-based nanoparticles for diagnostic applications have been extensively reported, they are only used for capturing and separating the target biomolecules. Quantitative detection of the target analyte was then evaluated by additional techniques such as Dynamic Light Scattering (DLS) [13], real-time

polymerase chain reactions (PCR) [17], surface-enhanced raman scattering (SERS) [18-20], fluorescence [23], magnetic relaxation switching [22] as well as ELISA [21,24] which need expensive instruments and highly skilled operators.

In prior work, a biocompatible zwitterionic copolymer, namely poly[(methacrylic acid)-co-(2-methacryloyloxyethyl phosphorylcholine)] (PMAMPC), was applied for the synthesis of the $Fe_3O_4$NPs by an in situ coating method, yielding PMAMPC-$Fe_3O_4$NPs. The success was relied on the ability of the carboxylate ions of the methacrylate units in the copolymer in chelating to Fe atoms. In aqueous media at neutral pH, the PMAMPC-$Fe_3O_4$NPs exhibited excellent long-term colloidal stability and had good biocompatibility. Being coated with the copolymer having a well-known antifouling component of PMPC, the PMAMPC-$Fe_3O_4$NPs also showed low non-specific adsorption of both positively and negatively charged proteins. By using EDC/NHS coupling chemistry, biomolecular probes can be conjugated to the carboxyl groups available on the MNPs coated with PMAMPC. Without the need for centrifugation, the target molecule can simply be captured and separated using an external magnetic field, showing the strong potential for biomagnetic separation [27].

In this research, the investigation of using PMAMPC-MNPs for instrument-free biomolecular detection was demonstrated. The concept of detection is based on the MNPs aggregation induced by specific interactions of complimentary biological components. Biotin and streptavidin (SA) were selected as models of specific probe and target molecule, respectively. Using the specific interactions of biotin-conjugated PMAMPC-MNPs and SA, the aggregation of nanoparticles is clearly observed by the naked eye without the requirement for any special equipment. Unlike the work previously reported by others [10-12,14-16], a magnetic field can induce aggregation, providing rapid detection. Additionally, the detection of target analytes in human serum samples was also demonstrated. We also explored the effects of variables such as the number of conjugated biotin, the amount of nanoparticles and the serum concentration on the detection efficiency of the assay.

## 2. Experimental

### 2.1 Materials

Ferrous chloride tetrahydrate ($FeCl_2{\cdot}4H_2O$), ferric chloride hexahydrate ($FeCl_3{\cdot}6H_2O$), ammonium hydroxide solution ($NH_4OH$, 28%w/v) phosphate buffer saline (PBS), streptavidin (SA), bovine serum albumin (BSA), 1-(3-(dimethylamino) propyl)-3-ethylcarbodiimide hydrochloride (EDC), N-hydroxysuccinimide (NHS), and streptavidin were purchased from Sigma-Aldrich (Singapore). Amine-PEG2-biotin (NH2-biotin) was purchased from Thermo Fisher Scientific (USA). Control human serum (HumaTrol N) was purchased from Human (Germany). Poly[(methacrylic acid)-co-(2-methacryloyloxyethyl phosphorylcholine)] (PMAMPC) having copolymer composition of 37:63 (PMA:MPC) and molecular weight of 54.5 kDa were synthesized by RAFT polymerization following the reported procedure [28]. The rod neodymium magnet with a dimension of 0.9 cm × 9.0 cm × 0.9 cm was used to generate a magnetic field in detection experiment.

### 2.2 Characterization

The morphology and size distribution of the MNPs were evaluated using transmission electron microscopy (TEM, Philips TECNAI 20). Attenuated total reflection fourier transform infrared (ATR-FTIR) spectra were recorded by a PerkinElmer Frontier. UV-vis absorption spectra were obtained using an Analytik Jena SPECORD 210 Plus spectrophotometer.

### 2.3 Preparation of PMAMPC-MNPs

PMAMPC-MNPs were prepared according to a previously reported method [27]. In brief, 298 mg (1.10 mmol) of $FeCl_3{\cdot}6H_2O$ and 114 mg, (0.57 mmol) of $FeCl_2{\cdot}4H_2O$ were dissolved in DI water (20 mL) in a flask at room temperature under nitrogen atmosphere at 60°C. The solution was mechanically stirred at 750 rpm and 6 mL of $NH_4OH$ (28%w/v) was added. The solution changed from orange to black. The black colloidal mixture was stirred for 1 h before being added with 40 mg of PMAMPC and continuously stirred for another hour. By using a magnet, the black MNPs were separated and washed thoroughly with DI water to remove unreacted chemicals. The PMAMPC-MNPs were dispersed in distilled water and stored as aqueous colloidal suspensions.

### 2.4 Conjugation of PMAMPC-MNPs with biotin probe

The amino-modified biotin was used as a model biomolecular probe and conjugated to PMAMPC-MNPs (Figure 1(a). To conjugate the biotin via covalent coupling, the carboxyl groups of coated PMAMPC were first activated by an aqueous solution of EDC and

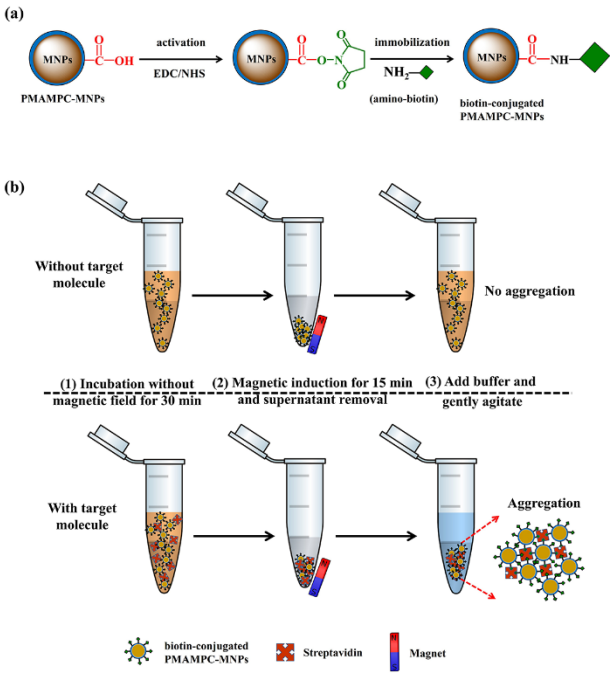


**Figure 1.** Schematic representation of the strategy for (a) conjugation of PMAMPC-MNPs with biotin probe and (b) detection of streptavidin by aggregation assay.

NHS. One hundred microliters of freshly prepared, mixed solution of EDC (50 mg·mL$^{-1}$) and NHS (50 mg·mL$^{-1}$) was added to 500 µL of aqueous suspension of PMAMPC-MNPs (10 mg·mL$^{-1}$). After being mixed for 30 min, the activated PMAMPC-MNPs were separated from the solution using a magnet and washed thoroughly with DI water. Then, the activated PMAMPC-MNPs were re-suspended in 500 µL of $NH_2$-biotin solution (10 mg·mL$^{-1}$) in DI water and incubated at room temperature (RT) overnight. After the incubation step, the biotin-conjugated PMAMPC-MNPs were separated with a magnet. The supernatant was collected and analyzed for the remaining $NH_2$-biotin by UV-vis spectrophotometry at 290 nm. The amount of conjugated biotin ($Q$, mg·g$^{-1}$) was calculated by the following equation.

$$Q = \frac{(C_0 - C_e)V}{m} \quad (1)$$

Where $C_0$ and $C_e$ are the $NH_2$-biotin concentrations before and after conjugation (mg·mL$^{-1}$), respectively. $V$ is the volume of the aqueous phase (mL), and $m$ is the weight of the nanoparticles (g). The biotin-conjugated PMAMPC-MNPs were washed and re-suspended in DI water.

### 2.5 Detection of streptavidin by biotin-conjugated PMAMPC-MNPs

The detection assay based on the nanoparticles aggregation is shown in Figure 1(b). Appropriate amounts of SA in PBS buffer (10 mM, pH 7.4) were added to the suspension of biotin-conjugated PMAMPC-MNPs (10 µL, 1 mg·mL$^{-1}$). The total volume of the solutions was adjusted to 100 µL. After thoroughly mixed, the solutions were incubated at room temperature for 30 min under gentle shaking. The nanoparticles were separated using a magnet for 15 min, washed and then redispersed in 100 µL of PBS buffer with gentle shaking for 1 min. To evaluate the selectivity of detection assay, the binding of biotin-conjugated PMAMPC-MNPs with bovine serum albumin (BSA) was also tested using the same protocol.

In addition, to demonstrate the applicability of the assay in real world samples, the detection of SA in human serum was conducted. Ten microliters of biotin-conjugated PMAMPC-MNPs suspension (1 mg·mL$^{-1}$) were added to 100 µL of human serum spiked with SA having a concentration in a range of 0 to 150 nM. The samples were incubated for 30 min at RT under gentle shaking. The nanoparticles were separated using a magnet for 15 min and redispersed in 100 µL of PBS buffer with gentle shaking for 1 min.

## 3. Results and discussion

### 3.1 Preparation and characterization of PMAMPC-MNPs and biotin-conjugated PMAMPC-MNPs

The magnetic nanoparticles coated with PMAMPC (PMAMPC-MNPs) were prepared by the *in situ* coating method. The success of surface coating of PMAMPC on MNPs was confirmed by ATR-FTIR (Figure 2(b)). The Fe-O stretching band was observed at 547 cm$^{-1}$ in the spectrum of uncoated MNPs (Figure 2(a)). The characteristic peaks of PMAMPC appearing at ~1700, ~1071 and 966 cm$^{-1}$ correspond to C=O, P=O and $N^+(CH_3)_3$ stretching vibrations, respectively.

Figure 3 illustrates the morphology of the uncoated MNPs and PMAMPC-MNPs determined by TEM. Both types of particles are spherical in shape with an average diameter of 12.3 ± 2.8 nm (n=100) for PMAMPC-MNPs and 12.9 ± 2.7 nm (n=100) for uncoated MNPs. The size of the nanoparticles was not significantly different. The coating of PMAMPC was considered as thin coating and hence, the coating process did not affect the average diameter and morphology of MNPs cores. However, pure MNPs began to aggregate and settle to the bottom of vial (indicated by red arrows in Figure 3(a) while PMAMPC-MNPs had a good colloidal stability (Figure 3(b)). This result showed that the colloidal stability of MNPs was improved by the PMAMPC modification.

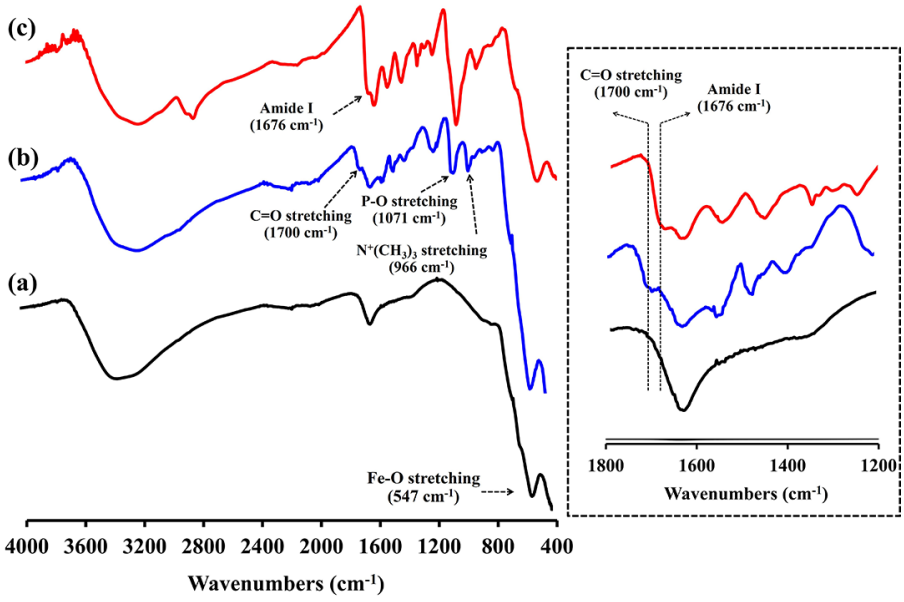


**Figure 2.** ATR-FTIR spectra of (a) MNPs, (b) PMAMPC-MNPs, and (c) biotin-conjugated PMAMPC-MNPs. Insert on the right of the figure are a magnification of ATR-IR spectra in the wavenumber range of 1200 cm$^{-1}$ to 1800 cm$^{-1}$.

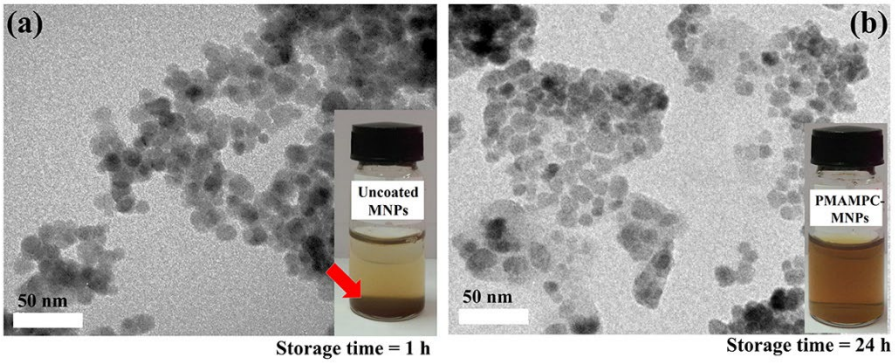


**Figure 3.** TEM images and photographs of suspensions (inset) of (a) MNP and (b) PMAMPC-MNPs.

To demonstrate the applicability of PMAMPC-MNPs for biomolecular detection, the biotin-streptavidin system was chosen as a model of recognition elements and analytes. This selection is attractive for the protein-ligand interaction study as the streptavidin (SA), a model biomarker protein is a protein with strong biotin-binding ability. Therefore, biotin conjugated to the MNPs was specifically capable of binding the SA target molecules or SA-labelled biomolecules in the samples. In addition, the well-known non-covalent bonding between biotin and SA has made it a preferable option in other biomolecular detection platforms [29,30]. After being activated by EDC/NHS chemistry, the carboxyl groups of the PMAMPC coated on the MNPs were conjugated with amino-functionalized biotin ($NH_2$-biotin). As evaluated by ATR-FTIR, the success of biotin conjugation was confirmed by the reduced intensity of the peak at 1700 $cm^{-1}$ assignable to C=O stretching vibration of carboxyl groups and the elevated intensity of the peak at 1676 $cm^{-1}$ assignable to amide peak, indicating that the carboxyl group of PMAMPC was converted to an amide linkage (Figure 2(c)). Inset of the ATR-FTIR is also provided in Figure 2 to demonstrate such changes. In addition, the peak around 2800 $cm^{-1}$ represented the C-H stretching of the polymer backbone was also appeared. The amount of carboxyl groups of the PMAMPC was decreased after biotin immobilization on PMAMPC-MNPs resulting in the decrease of broad O-H stretching peak around 2500 $cm^{-1}$ to 3500 $cm^{-1}$. Therefore, the C-H stretching peak was clearly observed after biotin-conjugated PMAMPC-MNPs (Figure 2(c)).

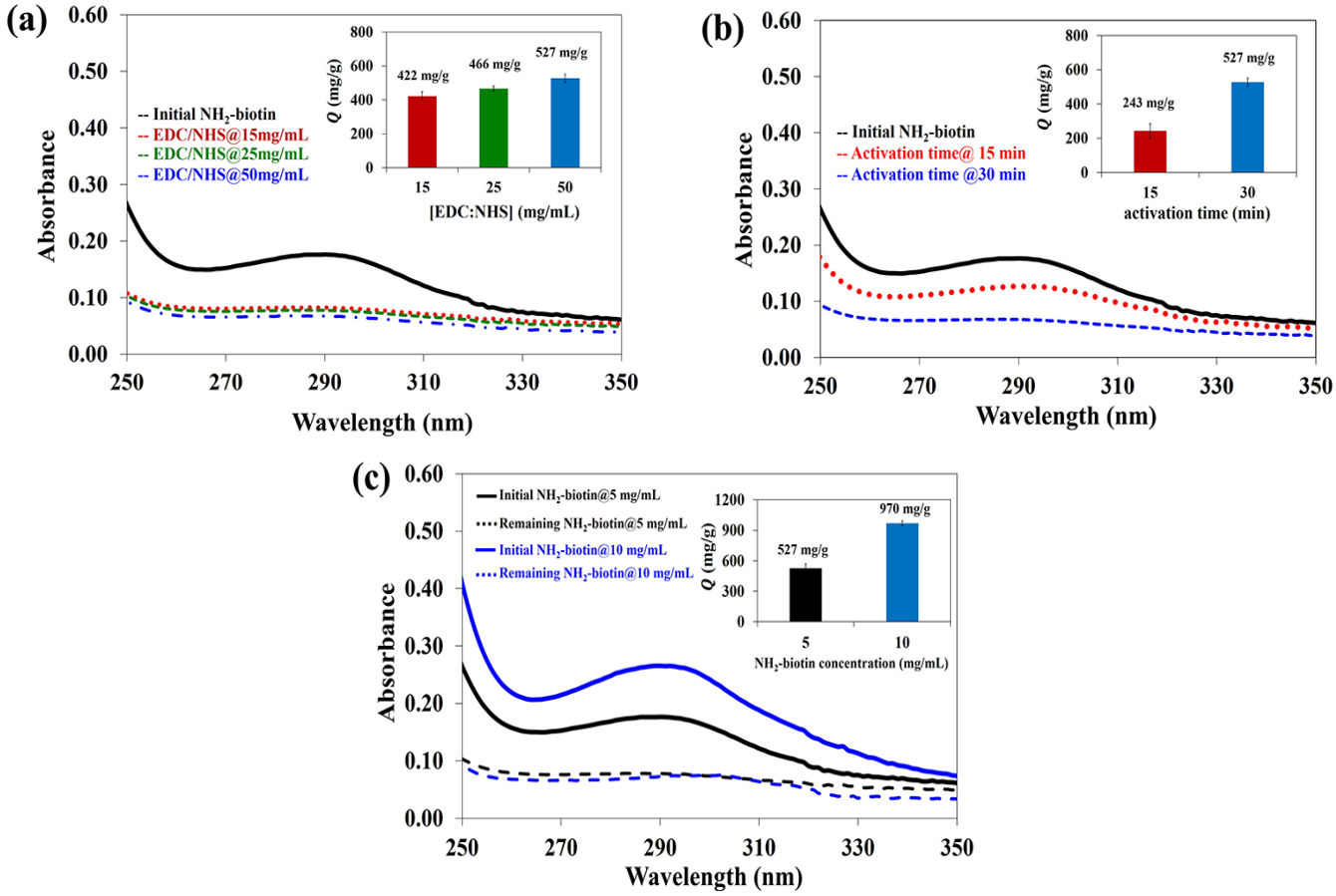


**Figure 4.** UV-vis data and Q values (insets) as a function of the (a) EDC/NHS concentration, (b) activation time, and (c) $NH_2$-biotin concentration.

The amounts of conjugated biotin per nanoparticles in term of mass ratio, $Q$ ($mg.g^{-1}$) was calculated by an indirect method in which the concentration of the remaining biotin in the supernatant was measured and compared with the initial biotin concentration. The decrease of the UV-vis absorption peak at 290 nm corresponding to biotin was observed upon biotin conjugation (Figure 4). The effect of the EDC/NHS concentration on the conjugation efficiency is also demonstrated in Figure 4(a). The $Q$ value increased with increasing EDC/NHS concentration. The activation time and $NH_2$-biotin concentration also affected the conjugation efficiency. The $Q$ value increased with the increasing activation time (Figure 4(b)) and $NH_2$-biotin concentration (Figure 4(c)). These results demonstrated that the conjugation efficiency of specific probes onto PMAMPC-MNPs depends on the degree of carboxyl group activation which can be controlled by the EDC/NHS concentration and activation time as well as the $NH_2$-biotin concentration.

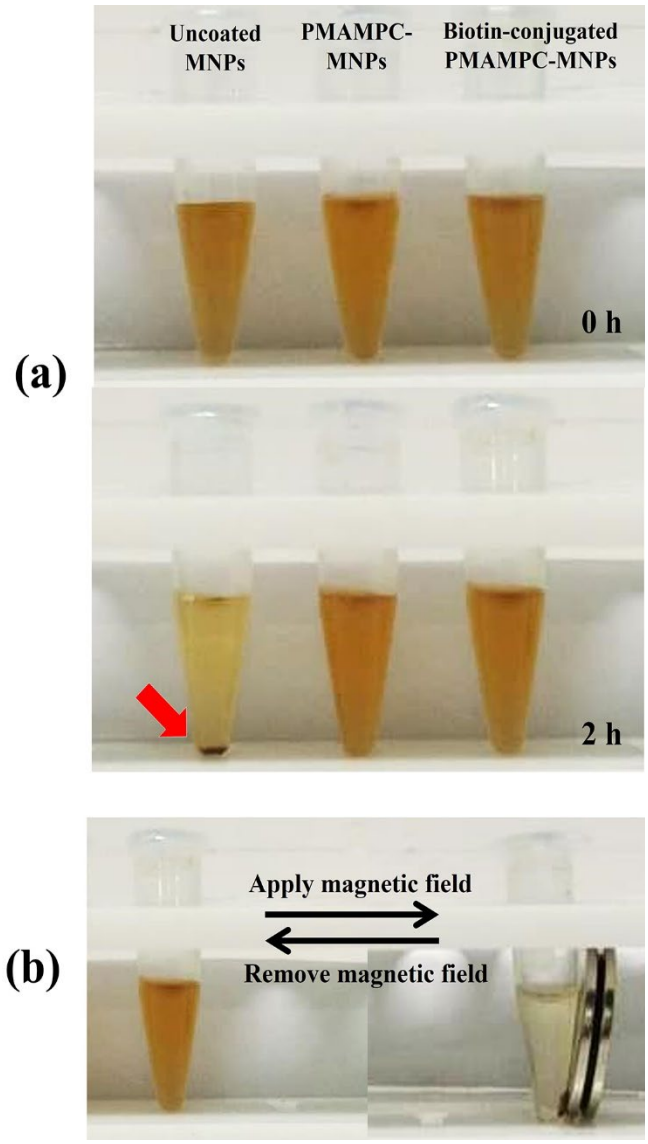


**Figure 5.** (a) Appearances of MNPs, PMAMPC-MNPs and biotin-conjugated PMAMPC-MNPs suspensions in 10% human serum without magnetic field. (b) Magnetic response of biotin-conjugated PMAMPC-MNPs suspensions with and without magnetic field.

As shown in Figure 5(a), a good dispersion was found in PMAMPC-MNPs and biotin-conjugated PMAMPC-MNPs for up to 2 h as opposed to the uncoated MNPs which were completely precipitated within 2 h. The result strongly supports that the modification of MNPs with a hydrophilic zwitterionic copolymer improves the colloidal stability of nanoparticles not only in aqueous solution but also in complex solution such as human serum. By applying an external magnetic field, the biotin-conjugated PMAMPC-MNPs could also simply be separated from the dispersion using an external magnetic field and readily dispersed back to the medium when external magnetic field was removed, showing an excellent magnetic response (Figure 5(b)).

### 3.2 Determination of streptavidin by biotin-conjugated PMAMPC-MNPs

The concept of an instrument-free detection assay used in this research relies on a key aspect of this aggregation phenomenon in that the biotin probes tethered on the PMAMPC-MNPs can bind with the target molecule, SA, inducing cross-linking between the nanoparticles. Another key aspect of the aggregation is that the size of nanoparticles (~12 nm) is equivalent to the molecular size of SA (~8 nm in diameter). As reported by previous work, when the size of nanoparticles is commensurate with the protein size, extended aggregates are formed [11,31]. However, the rate of aggregation to induce complete precipitation is slow. For example, in the case of gold nanoparticles, it takes over one night for obvious aggregation after contacting between probe-conjugated gold nanoparticles with the target molecules [11]. In this work, we also demonstrated the aggregation rate of biotin-conjugated PMAMPC-MNPs/SA complexes (Figure 6). For clearly visual aggregation, the measurement time for 12 h was required.

The slow aggregation rate would be improved by magnetic induction. As illustrated in Figure 7(a), the aggregation of the biotin-conjugated PMAMPC-MNPs/SA complex was not observed after the incubation with SA for 30 min. The magnetic field was induced to the complex for 5 min and 15 min to allow the aggregation (Figure 7(b)). After that the magnetic field was removed and the centrifuge tube was gently shaken. Apparently, the biotin-conjugated PMAMPC-MNPs/SA complex that was induced for 5 min was well redispersed and those with 15 min induction time still aggregate (Figure 7(c)). This result showed that SA could be detected by the magnet-induced aggregation for 15 min. Inter-particle crosslinking of biotin-conjugated PMAMPC-MNPs through SA is induced by the agglutination with a magnet.

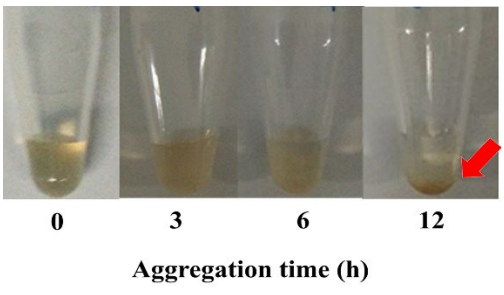


**Figure 6.** Appearances of biotin-conjugated PMAMPC-MNPs suspensions after incubation with 75 nM of SA at different times without a magnetic field.

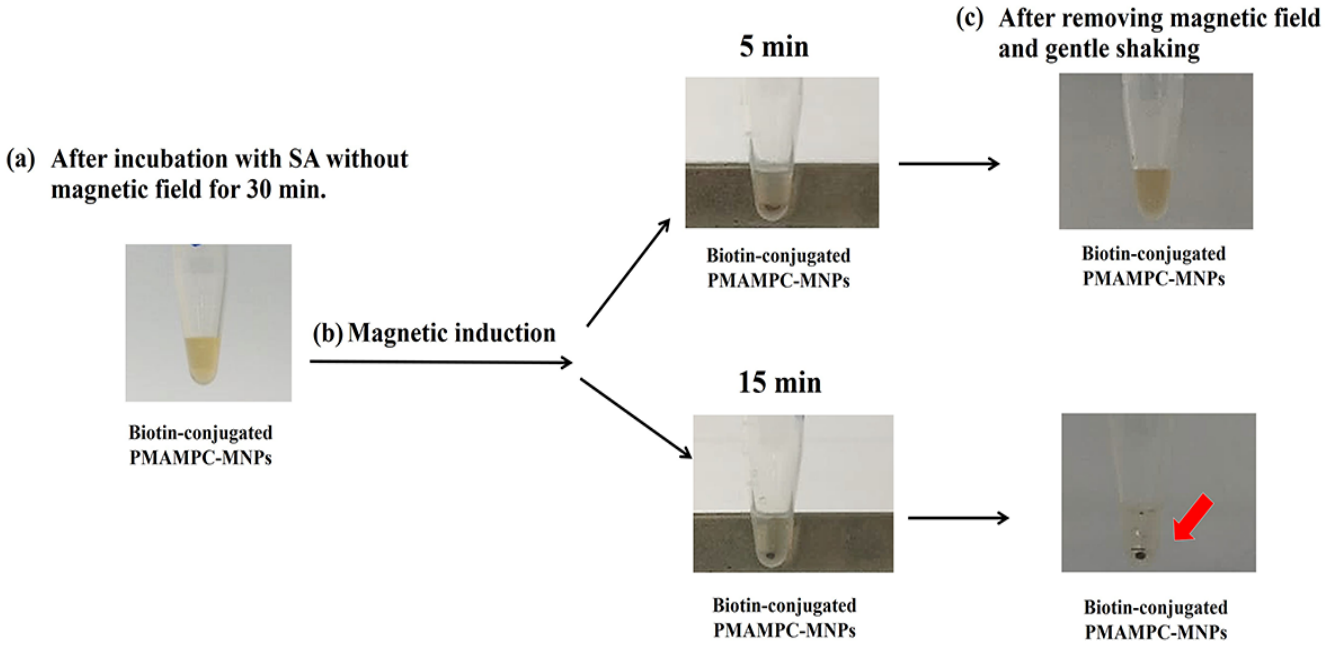


**Figure 7.** Appearances of the biotin-conjugated PMAMPC-MNPs suspensions (a) after incubation with SA without magnetic field, (b) magnetic induction in various time and (c) after removing magnetic field and gentle shaking. The concentration of the nanoparticles was 100 μg/mL and the concentrations of SA was 75 nM.

Figure 8(a-b) show the effect of nanoparticle concentration and amount of conjugated biotin on the detection efficiency, respectively. The nanoparticle concentration was varied from 50 $\mu g \cdot mL^{-1}$ to 500 $\mu g \cdot mL^{-1}$ while the SA concentration was kept constant at 150 nM. At high concentration of nanoparticles, no aggregation was observed, presumably because the ratio of SA per nanoparticle was very low and therefore inter-particle crosslinking between the nanoparticles could not form. At high values of $Q$ (970 $mg \cdot g^{-1}$) resulted in more aggregation of the nanoparticles than low values of $Q$ (527 $mg \cdot g^{-1}$). There is a greater possibility that high biotin content on the surface of biotin-conjugated PMAMPC-MNPs provides more binding sites for the SA molecules, resulting in numerous inter-particle crosslinks. A series of aggregation experiments were performed in which the concentration of SA was varied while the nanoparticle concentration was kept constant. Aggregation was observed at SA concentration ranging from 15 nM to 300 nM. At concentration of SA lower than 15 nM, no aggregation was observed, presumably because very few inter-particle crosslinks could form (Figure 9(a)). To confirm that this aggregation occurred by the specific binding between biotin conjugated on the MNPs and SA molecules, the non-biotin conjugated nanoparticles (PMAMPC-MNPs) were tested for SA detection with the same protocol. As expected, the good dispersion of PMAMPC-MNPs was maintained even in contact with high concentrations of SA (Figure 9(b)). This result indicated that there was no binding between PMAMPC-MNPs and SA because there were no conjugated biotin on the surface of PMAMPC-MNPs. Thus, PMAMPC-MNPs can readily disperse after removing the magnet. To evaluate the specificity of the assay, the detection was also performed on non-targeted molecules, BSA having a negative charge and a molecular weight (66 kDa) similar to that of streptavidin. Figure 7(c) showed that the aggregation of biotin-conjugated PMAMPC-MNPs was not observed even with high concentrations of BSA, confirming the specificity of this developed assay.

### 3.3 Determination of streptavidin in human serum

To demonstrate the potential of the developed assay for diagnostic applications, biotin-conjugated PMAMPC-MNPs were used to measure the SA in human serum representing a typical biological fluid. Human serum is a yellow liquid component of blood. Approximately 7% of the serum contains hundreds of proteins including albumin, globulin, and fibrinogen [32]. The detection of 150 nM SA solution (equivalent to 10 $\mu g \cdot mL^{-1}$) in various diluted human serum was performed. The results illustrated in Figure 10(a) indicated that the aggregation of biotin-conjugated PMAMPC-MNPs/SA complexes was not affected by the biologically relevant matrix in human serum, even in undiluted human serum (100%). Aggregation of biotin-conjugated PMAMPC-MNPs possibly due to nonspecific binding (without SA) with other interferences in human serum was not observed, indicating the good dispersion of the nanoparticles (Figure 10(b)).

The limit of detection for detecting SA in human serum is demonstrated in Figure 10(c). The lowest concentration of SA that can be distinguished by the naked eye was 35 nM or equivalent to 2.5 $\mu g \cdot mL^{-1}$. It should be noted that the concentration of a target biomolecule is much lower than those of other interference proteins present in human serum. Therefore, the developed assay can be further applied for diagnostic screening test of SA-labelled biomolecular detection. Additionally, this agglutination platform could be applied to other biological element systems that the recognition element immobilized MNPs, often antibody, could be changed to recognize and establish links with target analyze to form aggregates.

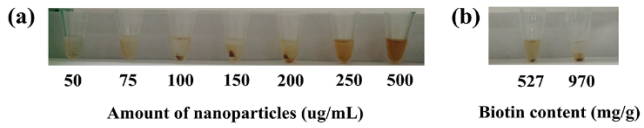


**Figure 8.** Appearances of the biotin-conjugated PMAMPC-MNPs suspensions after incubation with SA at (a) various concentrations of the nanoparticles and (b) different *Q* values. The concentration of SS was 150 nM and the magnetic induction time was 15 min.

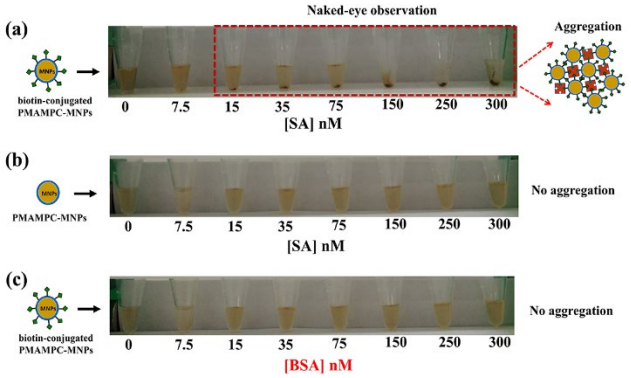


**Figure 9.** Appearances of (a) biotin-conjugated PMAMPC-MNPs suspensions and (b) PMAMPC-MNPs suspensions (non-biotin conjugated) after incubation with varied SA concentration, and (c) biotin-conjugated PMAMPC-MNPs suspensions after incubation with varied BSA concentration. The concentration of all nanoparticles was 100 $\mu g \cdot mL^{-1}$ and the magnetic induction time was 15 min.

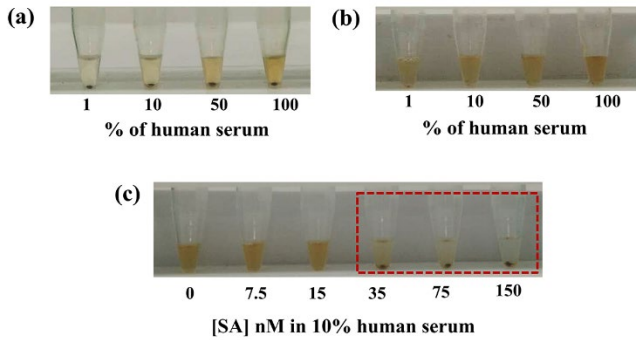


**Figure 10.** Appearances of the biotin-conjugated PMAMPC-MNPs suspensions in various diluted human serum (a) with 150 nM SA and (b) without SA and (c) in various SA concentrations using 10% human serum. The concentration of nanoparticles was 100 $\mu g \cdot mL^{-1}$ and the magnetic induction time was 15 min.

## 4. Conclusions

The instrument-free detection of target biomolecules in human serum using visual agglutination has been demonstrated. The capture probe conjugated MNPs exhibited excellent colloidal stability in human serum but could simply be separated upon applying an external magnetic field. Using the specific interaction of the biotin-SA linkage and the aid of a magnetic field, nanomolar concentrations of SA could be detected in a few minutes. Highly efficient SA detection assay in undiluted human serum can be established owing to the ability of the PMPC-containing copolymer used as a stabilizer for MNPs to resist nonspecific protein adsorption. This rapid and instrument-free assay would definitely become a valuable tool for point-of-care medical diagnosis especially in resource-poor settings.

## Acknowledgements

This work was supported by (i) Research Unit for Sensor Innovation (RUSI) for development and production of test kits, Burapha university (ii) the Center of Excellence for Innovation in Chemistry (PERCH-CIC) (iii) Science Innovation Facility, Faculty of Science, Burapha University. We thank Dr. Ron Beckett for English proof reading.

## References

[1] D. R Brenner, D. Scherer, K. Muir, J. Schildkraut, P. Boffetta, M. R Spitz, L. L. Marchand, A. T. Chan, E. L Goode, C. M Ulrich, and R. J. Hung "A review of the application of inflammatory biomarkers in epidemiologic cancer research," *Cancer Epidemiology, Biomarkers & Prevention,* vol. 23, no. 9, pp. 1729-1751, 2014.

[2] S.-E. Kim, Y. J. Kim, S. Song, K.-N. Lee, and W. K. Seong, "A simple electrochemical immunosensor platform for detection of apolipoprotein A1 (Apo-A1) as a bladder cancer biomarker in urine," *Sensors and Actuators B: Chemical,* vol. 278, pp. 103-109, 2019.

[3] K. Noi, A. Iwata, F. Kato, and H. Ogi, "Ultrahigh-frequency, wireless MEMS QCM biosensor for direct, label-free detection of biomarkers in a large amount of contaminants," *Analytical chemistry,* vol. 91, no. 15, pp. 9398-9402, 2019.

[4] B. Yuan, S. Schafferer, Q. Tang, M. Scheffler, J. Nees, J. Heil, S. Schott, M. Golatta, M Wallwiener, C. Sohn, T. Koal, B. Wolf, A. Schneeweiß, B. Burwinkel"A plasma metabolite panel as biomarkers for early primary breast cancer detection," *International journal of cancer,* vol. 144, no. 11, pp. 2833-2842, 2019.

[5] S.-H. Kwak, J.-S. Wi, J. Lee, C. Kim, and H.-K. Na, "Enhanced detection sensitivity through enzyme-induced precipitate accumulation in LSPR-active nano-valleys," *RSC advances,* vol. 12, no. 25, pp. 15652-15657, 2022.

[6] A. Uniyal, A. Pal, and Vivek Srivastava, "Advances in surface plasmon resonance–based biosensor technologies for cancer biomarker detection," *Biosensors and Bioelectronics,* vol. 197, p. 113767, 2022.

[7] S. Esmail, M. J. Knauer, H. Abdoh, C. Voss, B. Chin-Yee, P. Stogios, A. Seitova, A. Hutchinson, F. Yusifov, T. Skarina, E. Evdokimova, S. Ackloo, L. Lowes, B. D. Hedley, V. Bhayana, I. Chin-Yee and S. S-C. Li, "Rapid and accurate agglutination-based testing for SARS-CoV-2 antibodies," *Cell reports methods,* vol. 1, no. 2, p. 100011, 2021.

[8] J. Li, A. Concellón, K. Yoshinaga, Z. Nelson, Q. He, and T. M. Swager, "Janus emulsion biosensors for anti-SARS-CoV-2 spike antibody," *ACS Central Science,* vol. 7, no. 7, pp. 1166-1175, 2021.

[9] V. Kesarwani, J. A. Walker, E. C. Henderson, G. Huynh, H. McLiesh, M. Graham, M. Wieringa, M. M. B. Holl, G. Garnier, and S. R. Corrie, "Column agglutination assay using polystyrene microbeads for rapid detection of antibodies against SARS-CoV-2," *ACS Applied Materials & Interfaces,* vol. 14, no. 2, pp. 2501-2509, 2022.

[10] K. Sato, K. Hosokawa, and M. Maeda, "Rapid aggregation of gold nanoparticles induced by non-cross-linking DNA hybridization," *Journal of the American Chemical Society,* vol. 125, no. 27, pp. 8102-8103, 2003.

[11] Y. Iwasaki, T. Kimura, M. Orisaka, H. Kawasaki, T. Goda, and S.-i. Yusa, "Label-free detection of C-reactive protein using highly dispersible gold nanoparticles synthesized by reducible biomimetic block copolymers," *Chemical Communications,* vol. 50, no. 42, pp. 5656-5658, 2014.

[12] Y.-S. Borghei, M. Hosseini, M. Dadmehr, S. Hosseinkhani, M. R. Ganjali, and R. Sheikhnejad, "Visual detection of cancer cells by colorimetric aptasensor based on aggregation of gold nanoparticles induced by DNA hybridization," *Analytica chimica acta,* vol. 904, pp. 92-97, 2016.

[13] S. Iwasaki, H. Kawasaki, and Y. Iwasaki, "Label-free specific detection and collection of c-reactive protein using zwitterionic phosphorylcholine-polymer-protected magnetic nanoparticles," *Langmuir,* vol. 35, no. 5, pp. 1749-1755, 2018.

[14] E. Pinchon, F. Leon, N. Temurok, F. Morvan, J-J. Vasseur, M. Clot, V. Foulongne, J-F. Cantaloube, P. V. Perre, A. Daynès, J-P, Molès, and C. Fournier-Wirth, "Rapid and specific DNA detection by magnetic field-enhanced agglutination assay," *Talanta,* vol. 219, p. 121344, 2020.

[15] F. Leon, E. Pinchon, N. Temurok, F. Morvan, J-J Vasseur, M. Clot, V. Foulongne,[1] J-F. Cantaloube, P. V. Perre, J-P Molès, A. Daynès, and C. Fournier-Wirth, "Diagnostic performance of a magnetic field-enhanced agglutination readout in detecting either viral genomes or host antibodies in arbovirus infection," *Microorganisms,* vol. 9, no. 4, p. 674, 2021.

[16] F. Leon, E. Pinchon, C. Mayran, A. Daynès, F Morvan, J-P Molès, J-F Cantaloube, and C. Fournier-Wirth, "Magnetic field-enhanced agglutination readout combined with isothermal reverse transcription recombinase polymerase amplification for rapid and sensitive molecular detection of dengue virus," *Frontiers in chemistry,* vol. 9, p. 817246, 2021.

[17] Y. Mao, X. Huang, S. Xiong, H. Xu, Z. P. Aguilar, and Y. Xiong, "Large-volume immunomagnetic separation combined with multiplex PCR assay for simultaneous detection of Listeria monocytogenes and Listeria ivanovii in lettuce," *Food Control,* vol. 59, pp. 601-608, 2016.

[18] Y. Wan, Y. Sun, P. Qi, P. Wang, and D. Zhang, "Quaternized magnetic nanoparticles–fluorescent polymer system for detection and identification of bacteria," *Biosensors and Bioelectronics,* vol. 55, pp. 289-293, 2014.

[19] T. Xue, S. Wang, G. Ou, Y. Li, H. Ruan, Z. Li, Y. Ma, R. Zou, J. Qiu, Z. Shen, and A. Wu, "Detection of circulating tumor cells based on improved SERS-active magnetic nanoparticles," *Analytical Methods,* vol. 11, no. 22, pp. 2918-2928, 2019.

[20] R-S. Juang, W-T. Chen, Y-W. Cheng, K-S. Wang, R-J. Jeng, Z-L. Zeng, S-H. Liu, and T-Y. Liu, "Fabrication of in situ magnetic capturing and Raman enhancing nanoplatelets for detection of bacteria and biomolecules," *Colloids and Surfaces A: Physicochemical and Engineering Aspects,* vol. 648, p. 129189, 2022.

[21] Z. Zhang, Z. Wang, X. Wang, and X. Yang, "Magnetic nanoparticle-linked colorimetric aptasensor for the detection of thrombin," *Sensors and Actuators B: Chemical,* vol. 147, no. 2, pp. 428-433, 2010.

[22] Y. Xianyu, Y. Dong, Z. Wang, Z. Xu, R. Huang, and Y. Chen, "Broad-range magnetic relaxation switching bioassays using click chemistry-mediated assembly of polystyrene beads and magnetic nanoparticles," *ACS sensors,* vol. 4, no. 7, pp. 1942-1949, 2019.

[23] H. Zhang, C. Fu, S. Wu, Y. Shen, C. Zhou, J. Neng, Y. Yi, Y. Jin, and Y. Zhu, "Magnetic-capture-based SERS detection of multiple serum microRNA biomarkers for cancer diagnosis," *Analytical Methods,* vol. 11, no. 6, pp. 783-793, 2019.

[24] I.-H. Cho and J. Irudayaraj, "In-situ immuno-gold nanoparticle network ELISA biosensors for pathogen detection," *International journal of food microbiology,* vol. 164, no. 1, pp. 70-75, 2013.

[25] G. Bayramoglu, V. C. Ozalp, M. Oztekin, and M. Y. Arica, "Rapid and label-free detection of Brucella melitensis in milk and milk products using an aptasensor," *Talanta,* vol. 200, pp. 263-271, 2019.

[26] K. G. Neoh, and E. T. Kang, "Functionalization of inorganic nanoparticles with polymers for stealth biomedical applications," *Polymer Chemistry,* vol. 2, no. 4, pp. 747-759, 2011.

[27] S. Boonjamnian, T. Trakulsujaritchok, K. Srisook, V. P. Hoven, and P. N. Nongkhai, "Biocompatible zwitterionic copolymer-stabilized magnetite nanoparticles: a simple one-pot synthesis, antifouling properties and biomagnetic separation," *RSC advances,* vol. 8, no. 65, pp. 37077-37084, 2018.

[28] P. Akkahat, S. Kiatkamjornwong, S.-i. Yusa, V. P. Hoven, and Y. Iwasaki, "Development of a novel antifouling platform for biosensing probe immobilization from methacryloyloxyethyl phosphorylcholine-containing copolymer brushes," *Langmuir,* vol. 28, no. 13, pp. 5872-5881, 2012.

[29] E. A Gould, A. Buckley, and N. Cammack. "Use of the biotin-streptavidin interaction to improve flavivirus detection by immunofluorescence and ELISA tests," *Journal of virological methods,* no. 1, pp. 41-48, 1985.

[30] M. Zhu, G. Xue, H. Yonghong, O. Weijun, and W. Yakun. "Streptavidin-biotin-based directional double Nanobody sandwich ELISA for clinical rapid and sensitive detection of influenza H5N1," *Journal of translational medicine,* vol. 12, no. 1, pp. 1-10, 2014.

[31] M. De, O. R. Miranda, S. Rana, and V. M. Rotello, "Size and geometry dependent protein–nanoparticle self-assembly," *Chemical communications,* no. 16, pp. 2157-2159, 2009.

[32] A. Blanco, and G. Blanco, *Medical biochemistry*. Academic Press, 2017.